Electronic Supplementary Material (ESI) for RSC Advances.

Supporting Information

g-C_3N_4/rGO Nanocomposite As Highly Efficient Metal-Free Photocatalyst for Direct C-H Arylation under Visible Light Irradiation

Xiaohui Cai, Hanwen Liu, Lihua Zhi, Huang Wen, Ailing Yu, Lianhua Li, Fengjuan Chen*, Baodui Wang*

[1]State Key Laboratory of Applied Organic Chemistry and Key Laboratory of Nonferrous Metal Chemistry and Resources Utilization of Gansu Province and Lanzhou University, Lanzhou, Gansu, 730000 (P.R. China).

E-mail: chenfj@lzu.edu.cn, wangbd@lzu.edu.cn

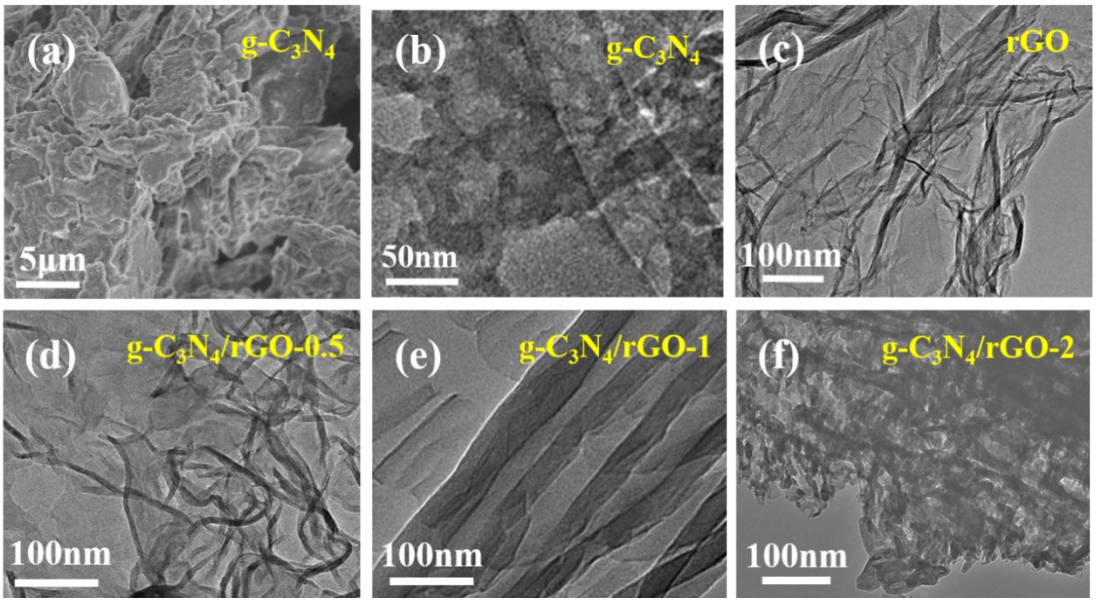

Figure S1. (a) SEM image of pure g-C_3N_4; (b) TEM image of pure g-C_3N_4; (c) TEM image of rGO; (d) TEM image of g-C_3N_4 /rGO-0.5 nanocomposite; (e) TEM image of g-C_3N_4 /rGO-1nanocomposite; (f) TEM image of g-C_3N_4 /rGO-2 nanocomposite. Both of the SEM and TEM images of pristine g-C_3N_4 show that the prepared sample is composed of many nanosheets stacked on each other and its structure has typical fold layers. The TEM image of rGO displays two-dimensional sheets with chiffon-like ripples and wrinkles, which make the rGO possess a large specific surface area. The g-C_3N_4/rGO nanocomposite with different rGO ratios were obtained by tuning the rGO weight ratio from 0.5 to 2.0 wt% in precursors. TEM images of g-C_3N_4/rGO

nanocomposite with different rGO ratios indicate that all of the nanocomposites show the lamellar structures.

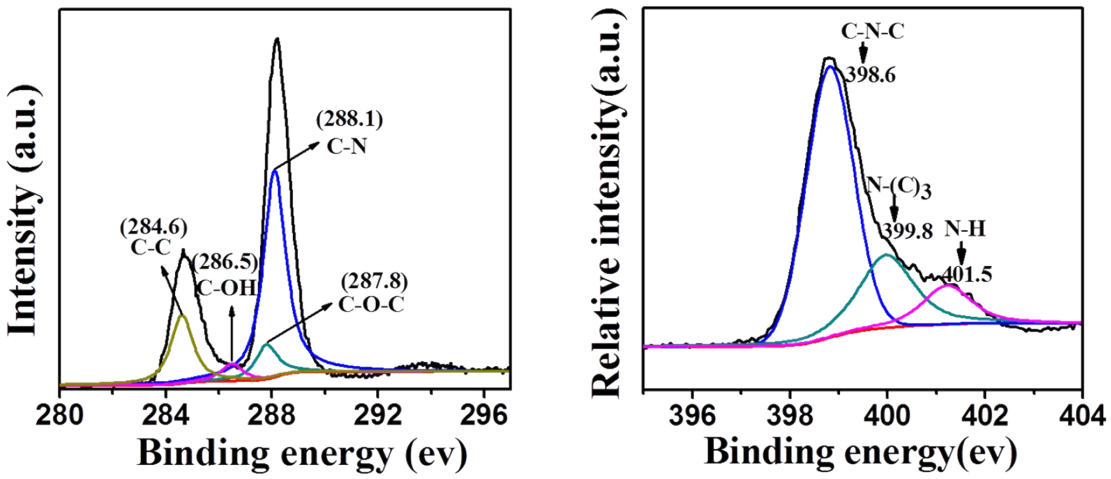

Figure S2. (a) High-resolution C 1s XPS spectra of the g-C_3N_4/rGO-1 nanocomposite. (b) High-resolution scans for N 1s of the g-C_3N_4/rGO-1 nanocomposite. Figure S2 (a) shows that the sample has four peaks at 284.6, 286.5, 287.8 and 288.1 eV which assigned to the carbon and sp^2 C–C bonds, C-OH, C-O-C and N=C-N_2, respectively.[1] The high resolution N 1s XPS spectra of g-C_3N_4/rGO nanocomposite could be fitted into three peaks centered at 398.6, 399.8 and 401.5 eV (Figure S2b).[1] The N 1s peaks at 398.6 and 399.8 eV corresponded to sp^2-hybridized aromatic N bonded to carbon atoms (C=N–C) and the tertiary N groups (N–$(C)_3$). Another, the weak peak at 401.5 eV indicated the existence of amino functional groups (C–N–H), which because of the defective condensation of the structures.

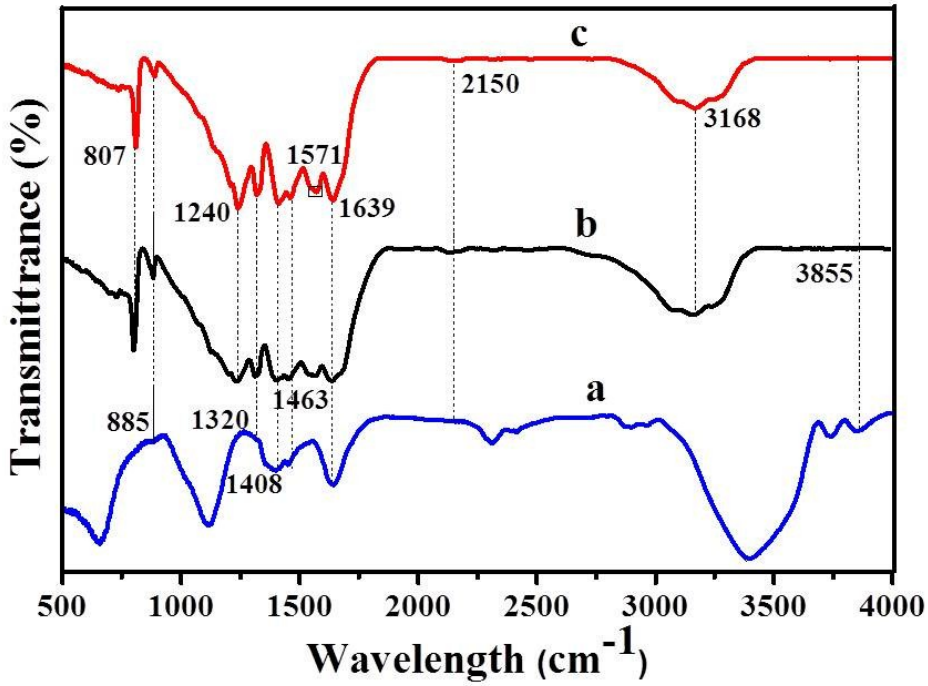

Figure S3. (a) The FTIR spectra of rGO; (b) The FTIR spectra of pure g-C_3N_4; (c) The FTIR spectra characterilization of g-C_3N_4/rGO-1 nanocomposite; For pure rGO, the peaks at 1068 and 1406 cm^{-1} are attributed to the C-O stretching vibrations and tertiary C-OH groups stretching, respectively. The absorptions at 1631 and 1723 cm^{-1} can be assigned to the O-H bending vibration of epoxide groups and skeletal ring and the C=O stretching of COOH groups, respectively. The absorptions in the 1200-1650 cm^{-1} region correspond to the typical stretching modes of CN heterocycles of pure g-C_3N_4 (Figure S3b). The FTIR characterlization of g-C_3N_4/rGO nanocomposite indicates that the bands of pure g-C_3N_4 still remain, and a new peak emerges at 1571 cm^{-1}, which is attributed to the skeletal vibration of the rGO sheets,[2] indicating the presence of these sheets in the g-C_3N_4/rGO-1 nanocomposite.

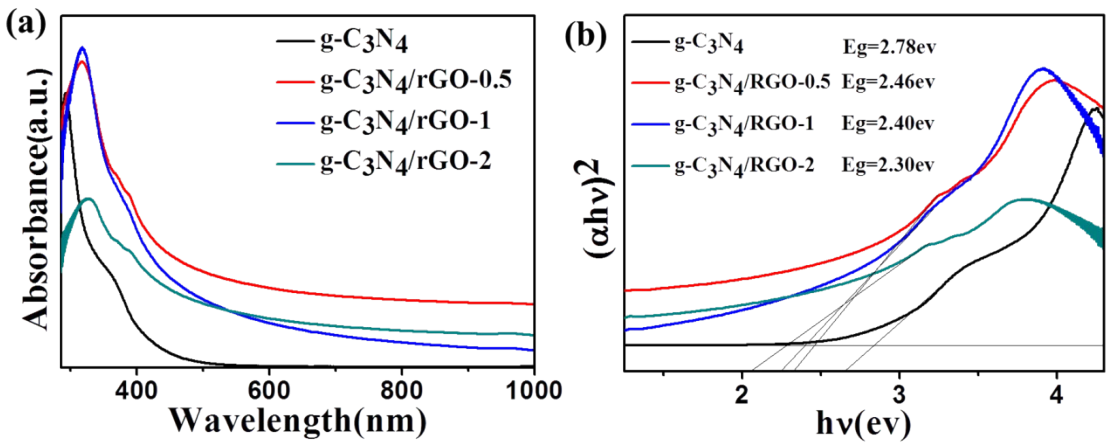

Figure S4. (a) UV-vis diffuse reflectance spectras of the g-C_3N_4 and g-C_3N_4/rGO nanocomposite; (b) The plots of transformed Kubelka-Munk functions versus the light energy.

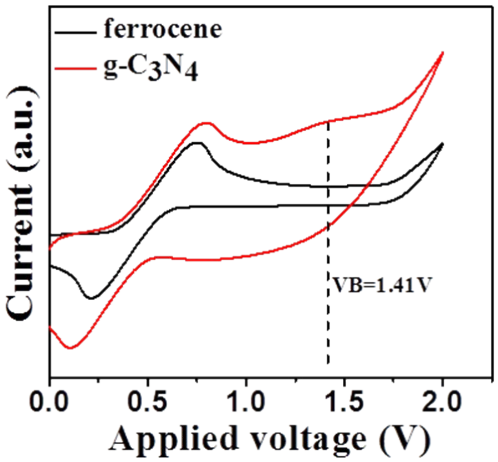

FigureS5: The cyclic voltammograms of the oxidation potential of ferrocene (black) as the internal standard to calibrate the measurements and cyclic voltammetry of g-C_3N_4.

The valence band (VB) of individual g-C_3N_4 was determined to be 1.41 eV(FigureS5). Based on the bandgap date of the nanocomposites obtained by UV-vis diffuse reflectance spectra (Figure2d), the calculated valence band potentials (E_{CB}) for g-C_3N_4 is -1.37 eV. rGO has not absorption of light(Figure2c), so there is not corresponding band gap. Using ferrocene as the reference materials, the VB energy levels of the inorganic semiconductors can be calculated using the following equation: $E_{VB} = (E_{red} - E_{ferrocene})$, where $E_{ferrocene} = 0.3eV$.[3,4]

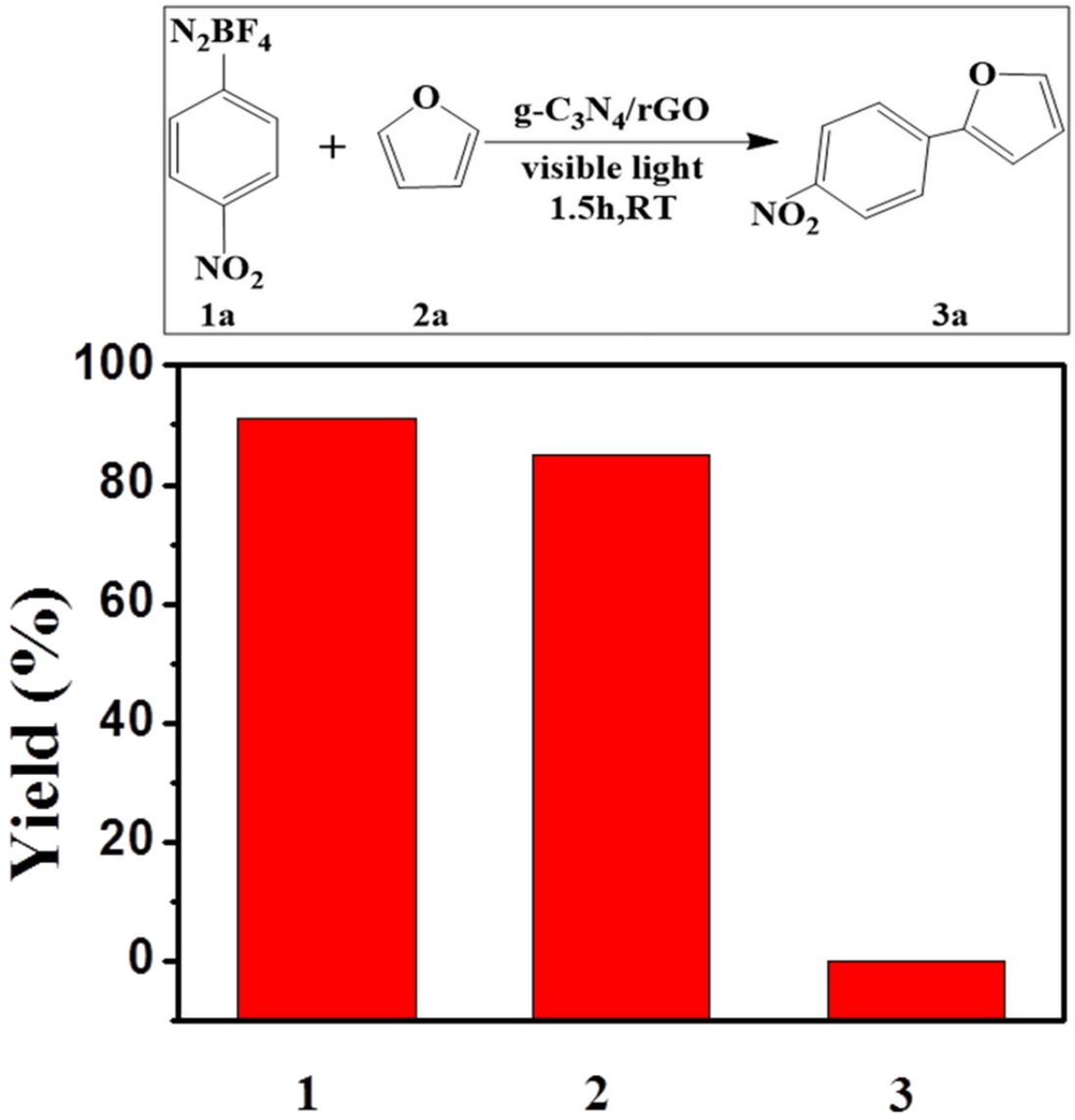

Figure S6. The control experiments with different radical scavengers for the photocatalytic reaction. Reaction conditions: (1) 0.1 mmol **1a**, 4 mg g-C_3N_4/rGO nanocomposites, 1 mL DMF and 1 mL furan, irradiation with visible light for 1.5 h under nitroge atmosphere; (2) the reaction in the absence of 0.1mg EDIA as a scavenger of holes; (3) the reaction in the absence of 0.1mg 1,4-Benzoquinone as a scavenger. All the yields are determined by GC.

Radical Capturing Experiments

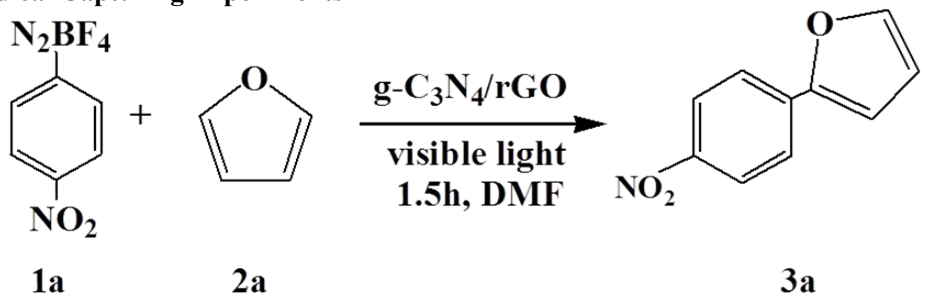

1a 2a 3a

(a) Reaction conditions: 0.1 mmol 1a, 4 mg g-C_3N_4/rGO nanocomposite, 1 mL furan, 1 mL DMF, irradiation with visible light for 1.5 h under nitrogen atmosphere.
(b) Reaction conditions: 0.1 mmol 1a, 4 mg g-C_3N_4/rGO nanocomposite, 1 mL DMF, 1 mL furan, 0.2 mmol 2,2,6,6-tetramethylpiperidinoxyl (TEMPO), irradiation with visible light for 1.5 h under nitrogen atmosphere.[5]

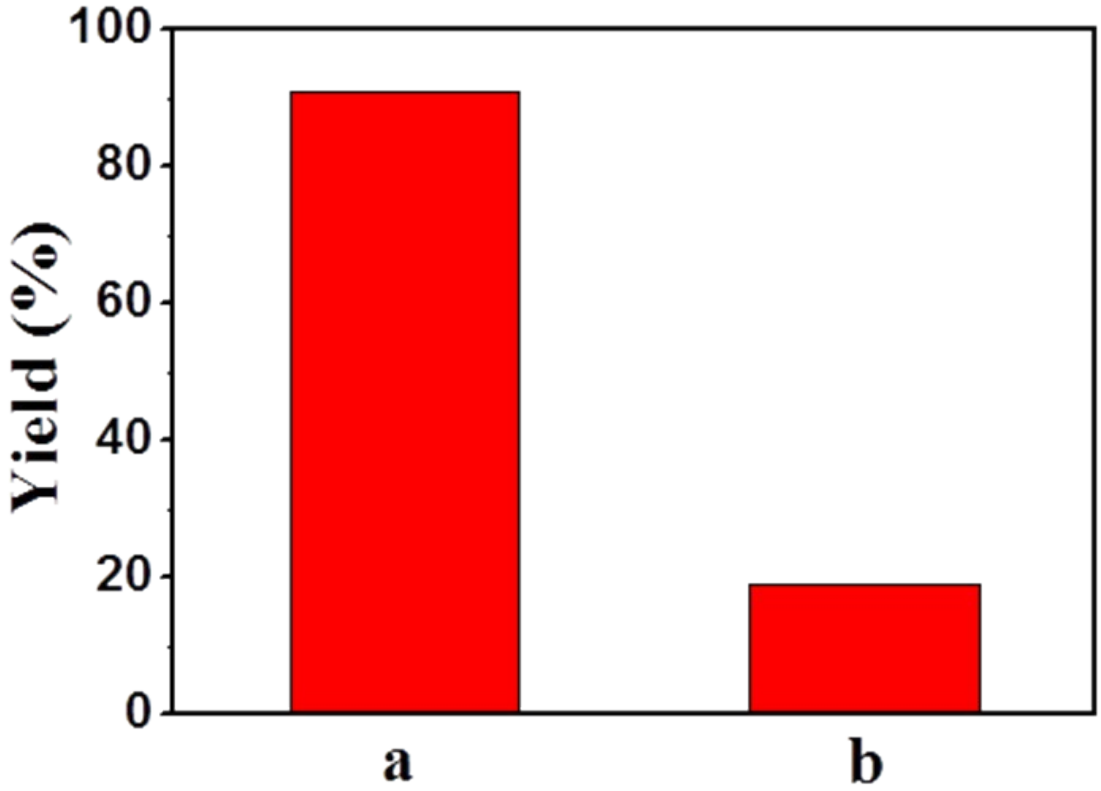

Figure S7. The control experiment to confirm the electron transfer mechanism for direct C-H arylation. (a) the target product yield without TEMPO; (b) the target product yield with TEMPO added.

Figure S8. The photo of g-C_3N_4 (a), g-C_3N_4 /rGO-1 (b) and g-C_3N_4 /rGO-2 (c).

products	g-C_3N_4/rGO	Eosin Y[5]	3DFe_3O_4@Cu_{2-X}S-MoS_2F[6]	TiO_2[7]
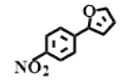	91%	85%	96%	90%
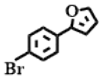	92%	84%	97%	90%
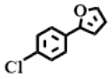	96%	74%	98%	94%
	88%	60%	90%	77%
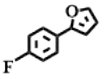	89%		98%	96%
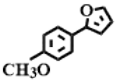	72%	54%	80%	79%
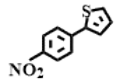	80%	70%	86%	83%
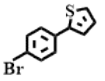	74%		77%	67%
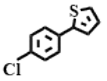	79%		86%	72%
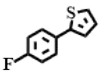	60%			

TableS1. The results obtained with direct arylation of heteroaromatics under visible-light irradiation at room temperature using metal-free g-C_3N_4/rGO nanocomposite as photocatalyst is compare with other photocatalysts reported.

Characterization of synthesized products:

2-(4-Nitrophenyl)furan[8]

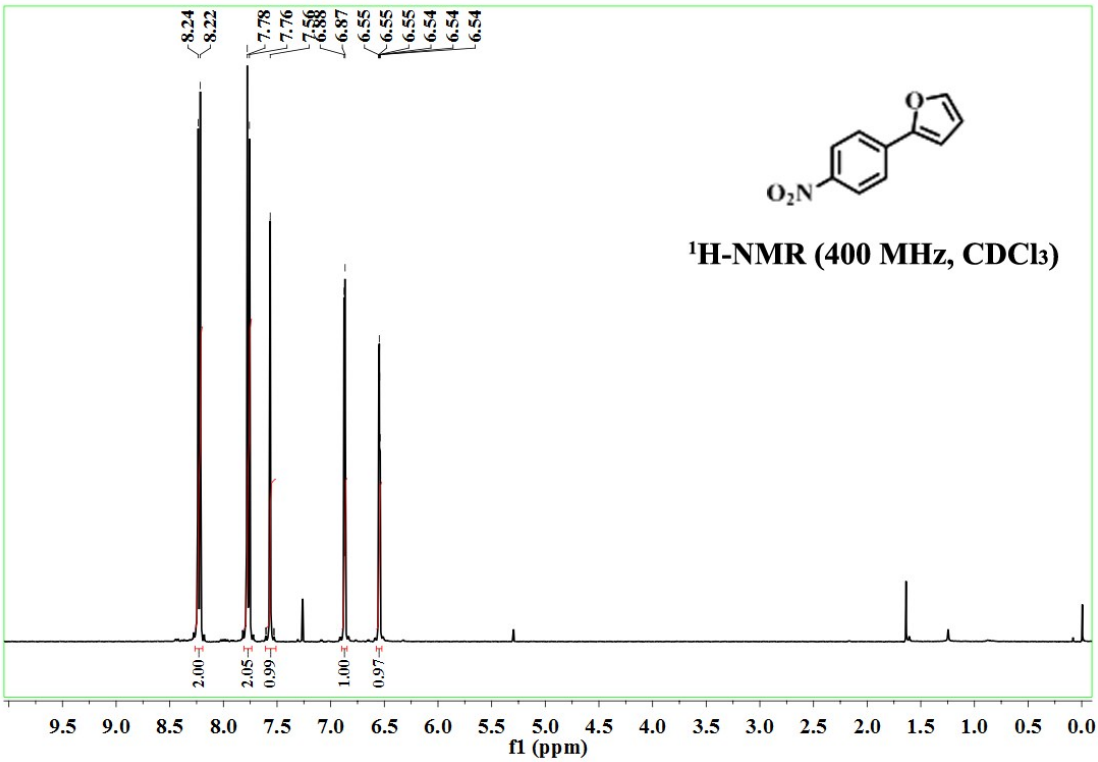

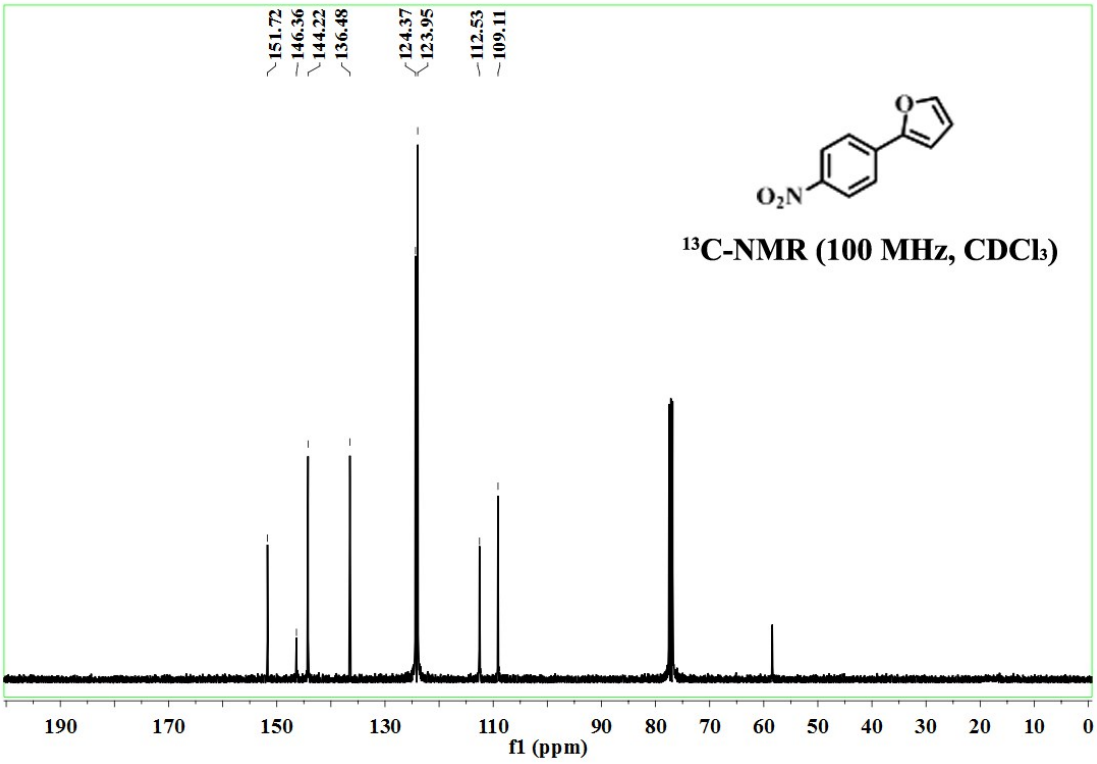

2-(4-Chlorophenyl)furan[8]

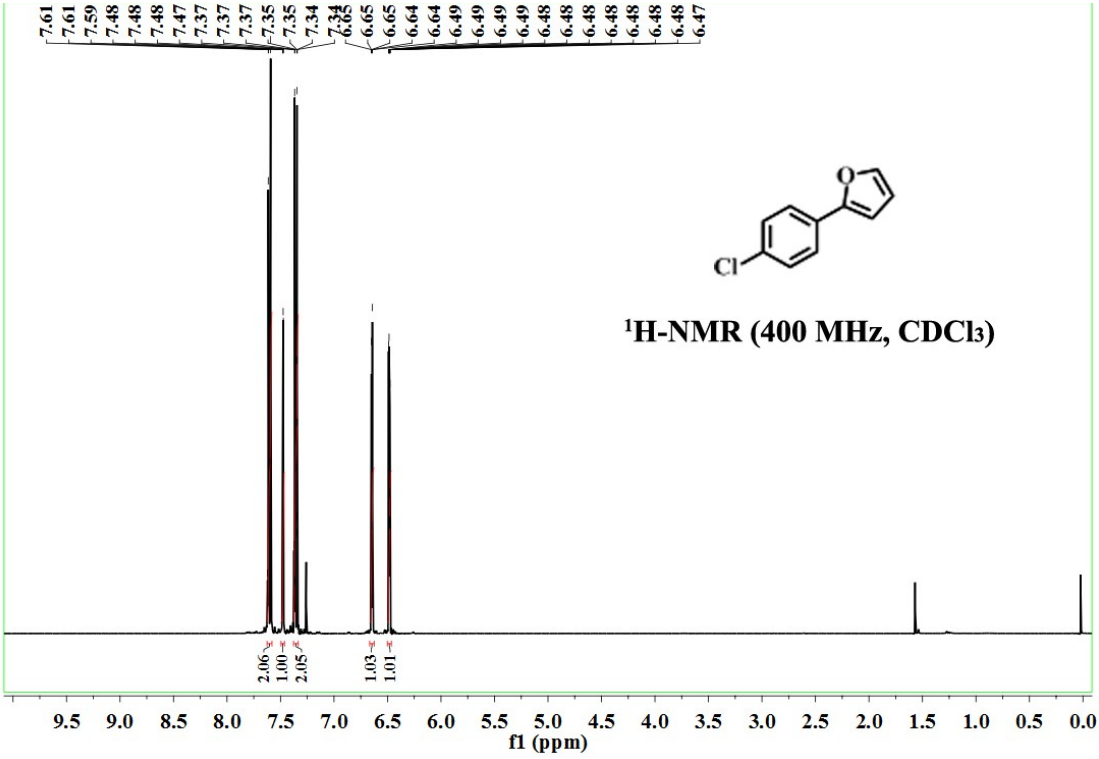

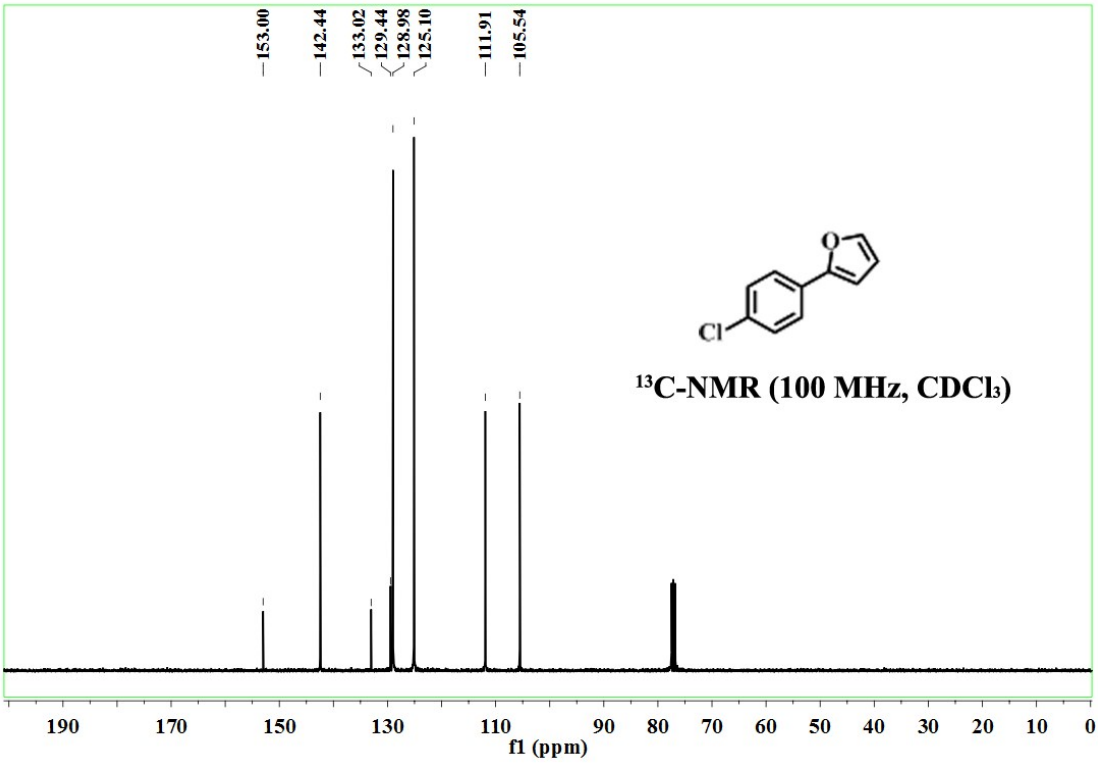

^{13}C-NMR (100 MHz, $CDCl_3$)

2-(4-Bromophenyl)furan[8]

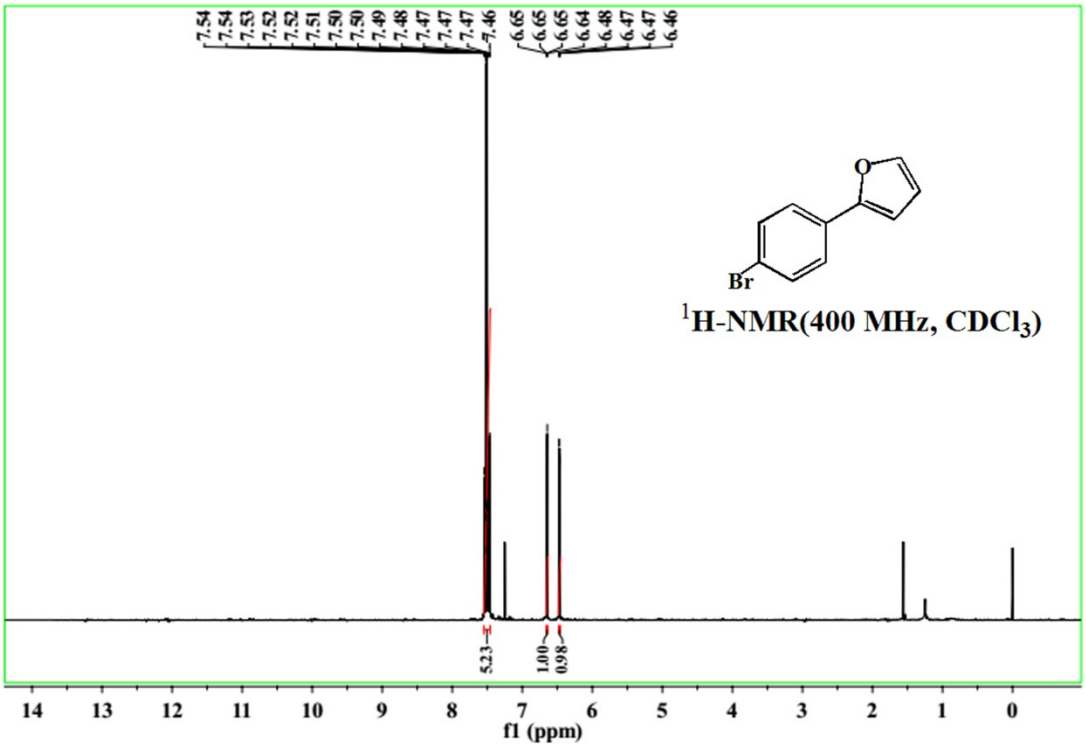

^{1}H-NMR(400 MHz, $CDCl_3$)

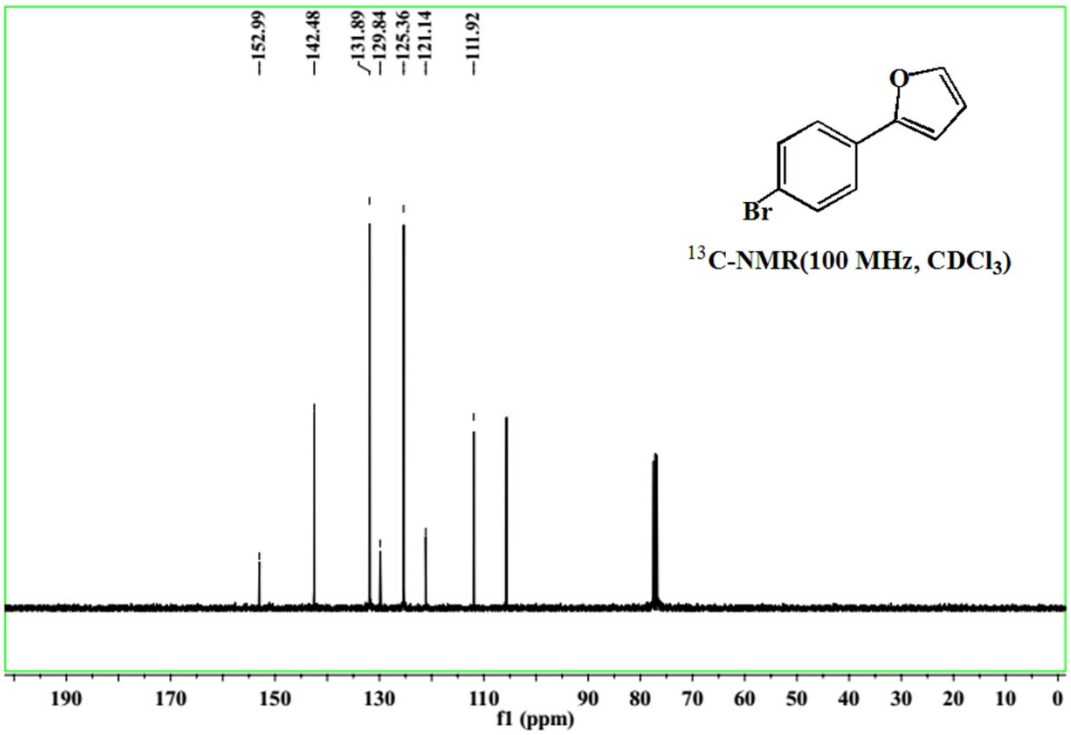

2-(4-Fluorophenyl)furan[9]

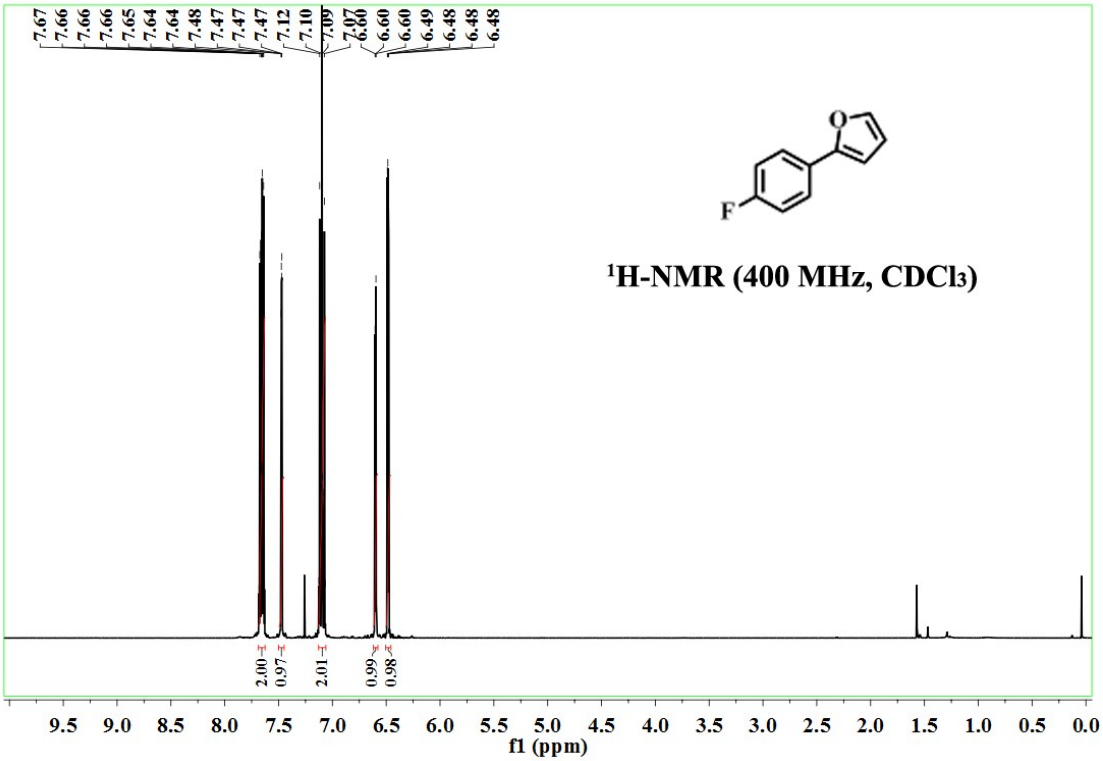

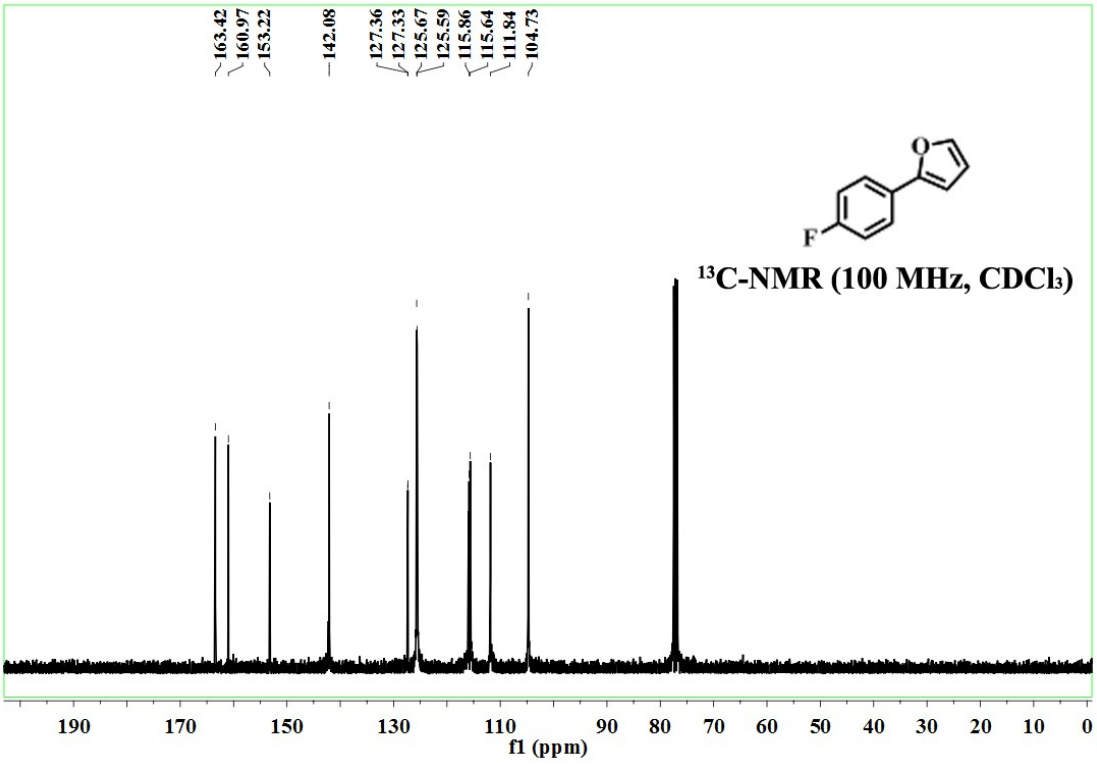

2-(4-Methoxyphenyl)furan[8]

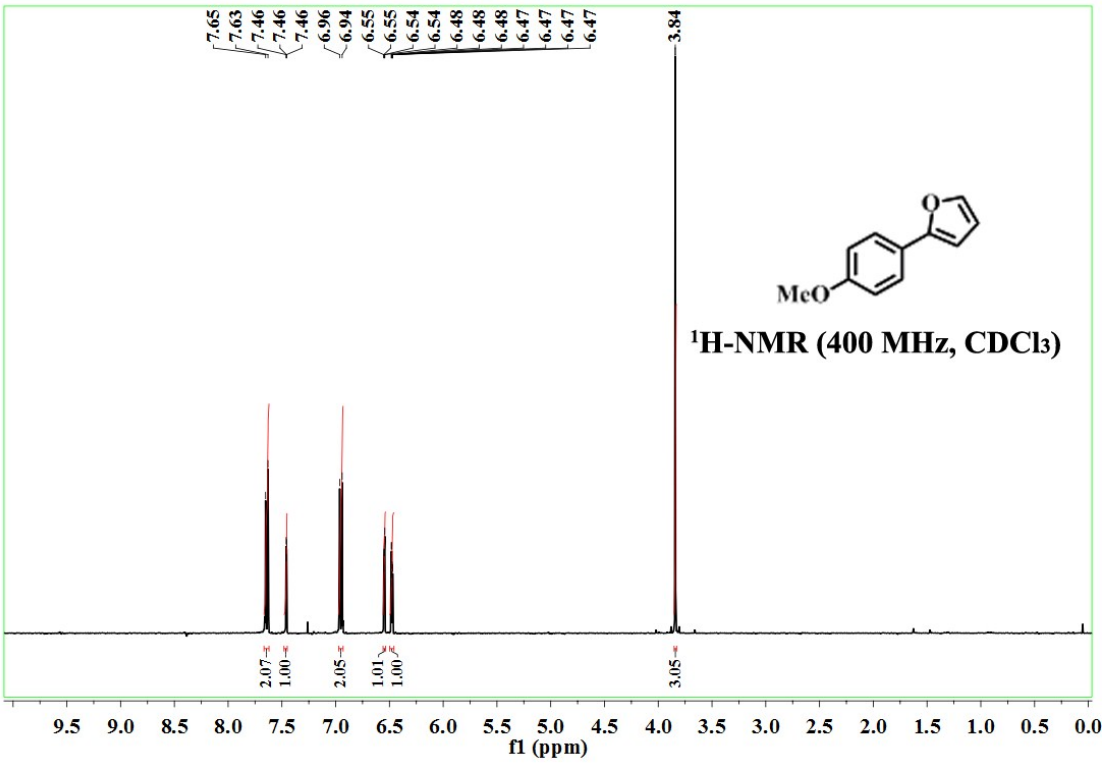

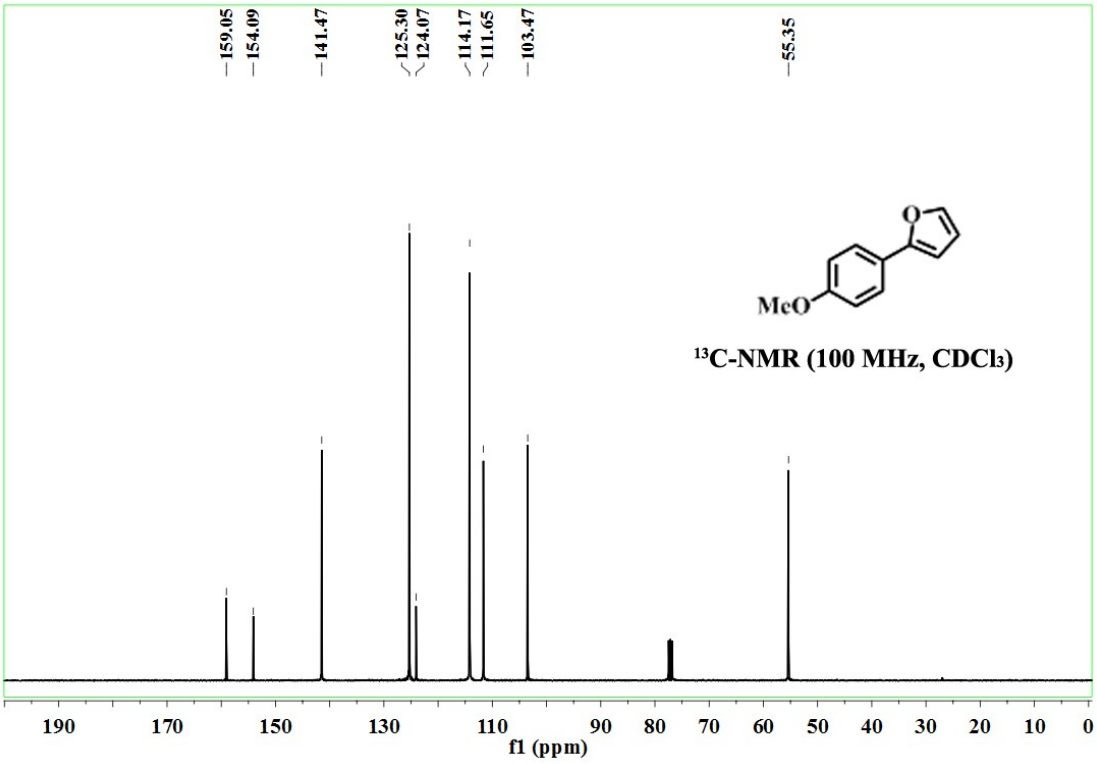

2-Phenylfuran[8]

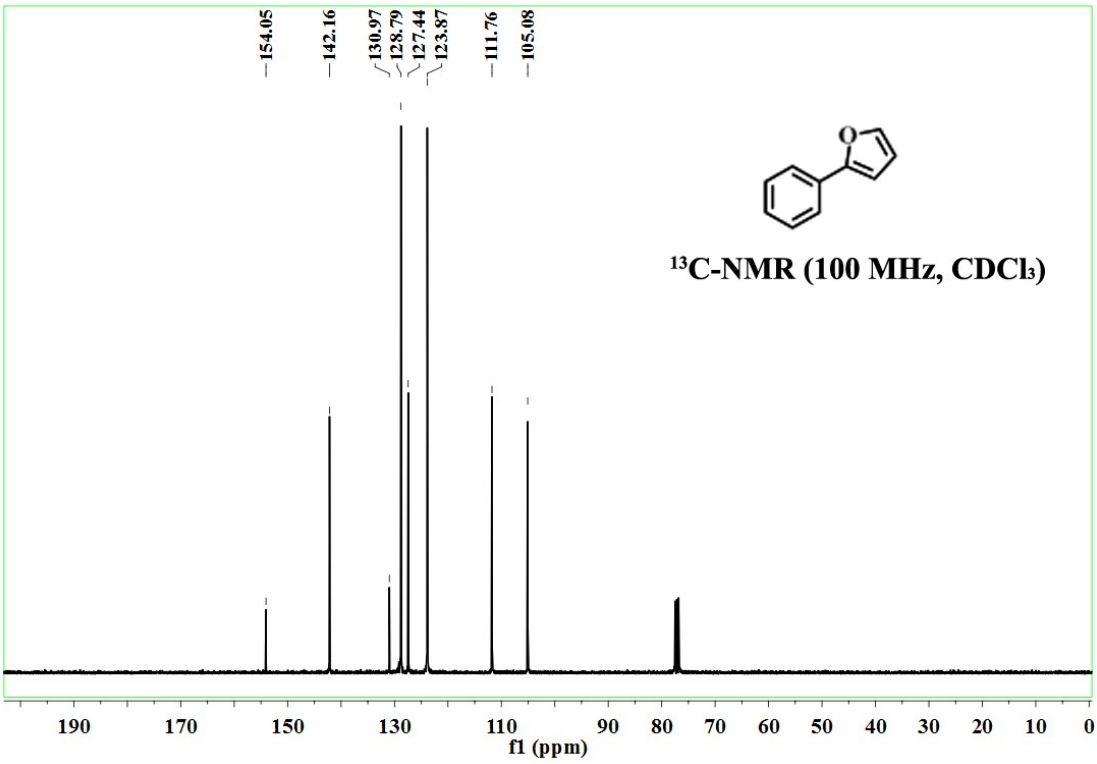

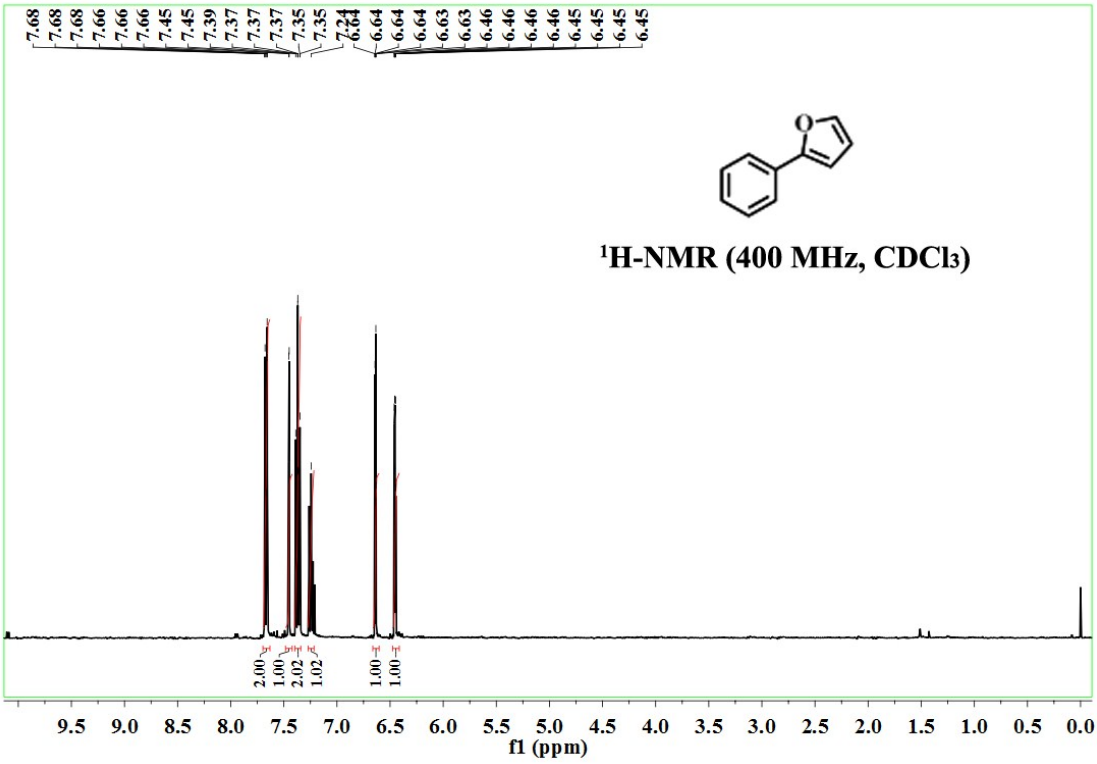

2-(4-Nitrophenyl)thiophene[10]

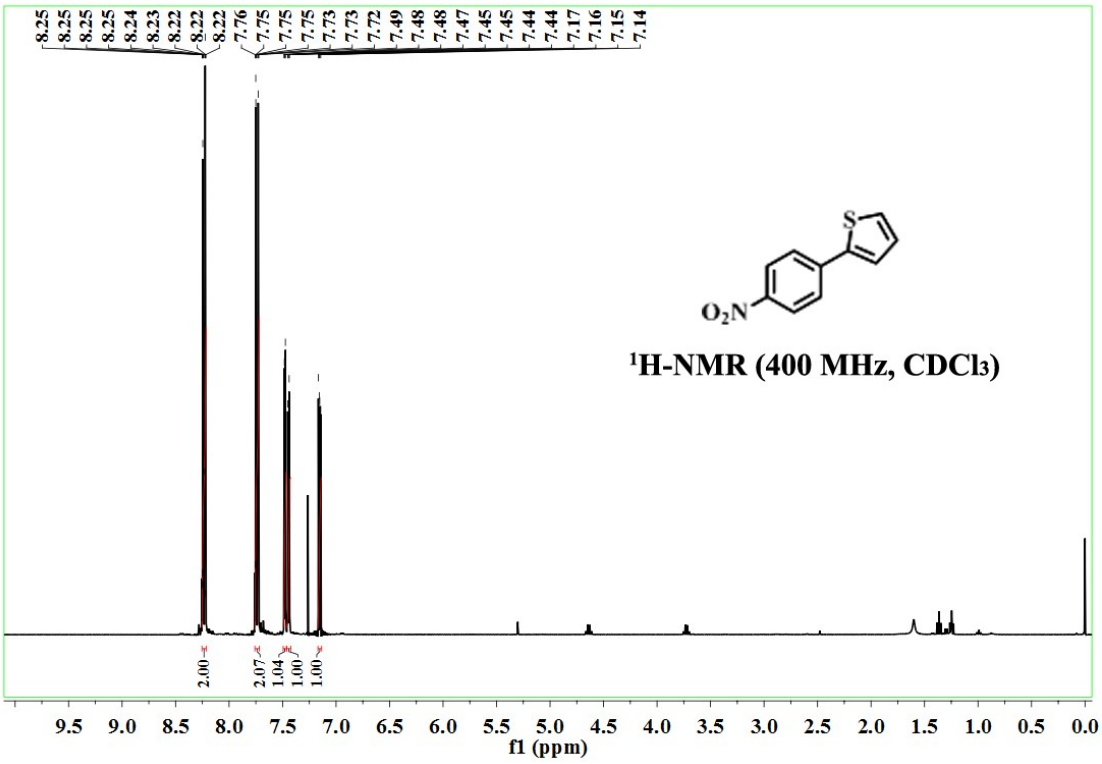

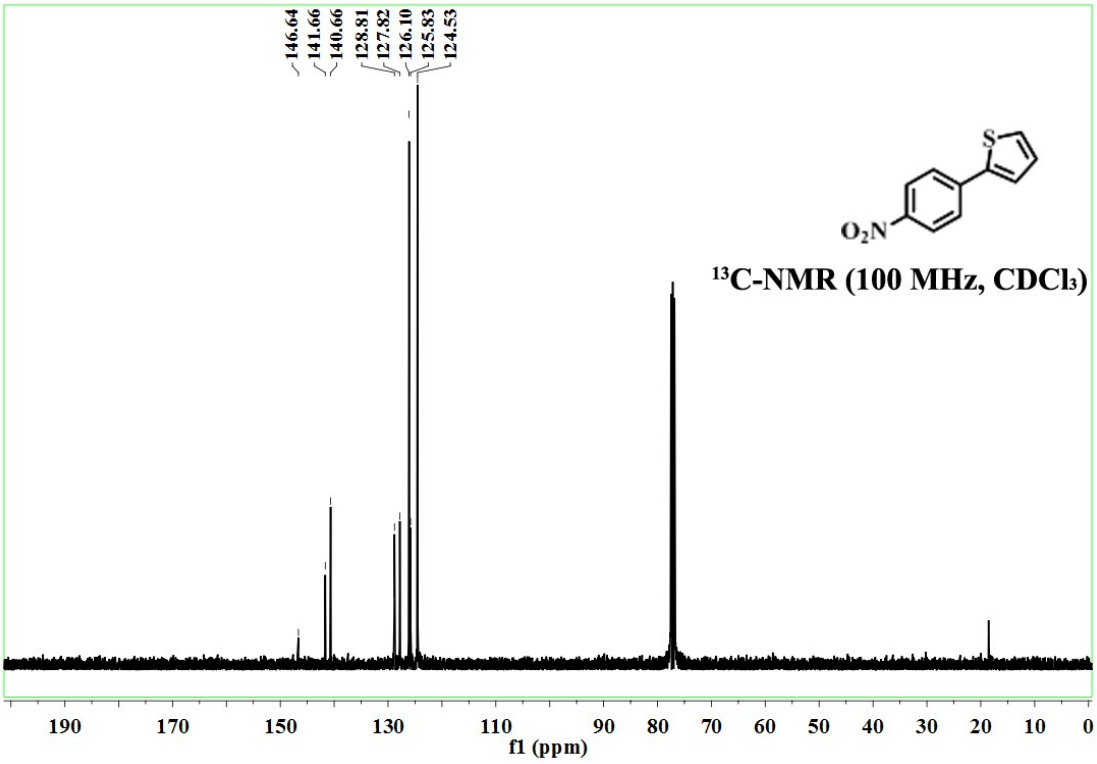

2-(4-Chlorophenyl)pyridine[11]

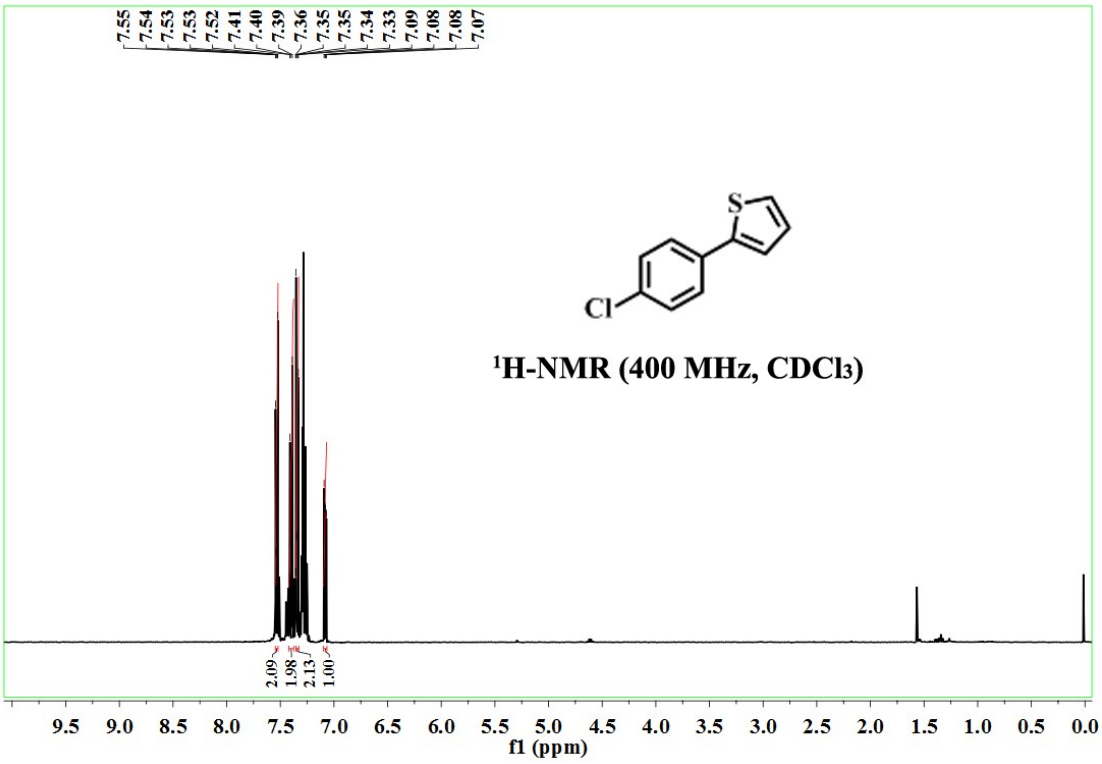

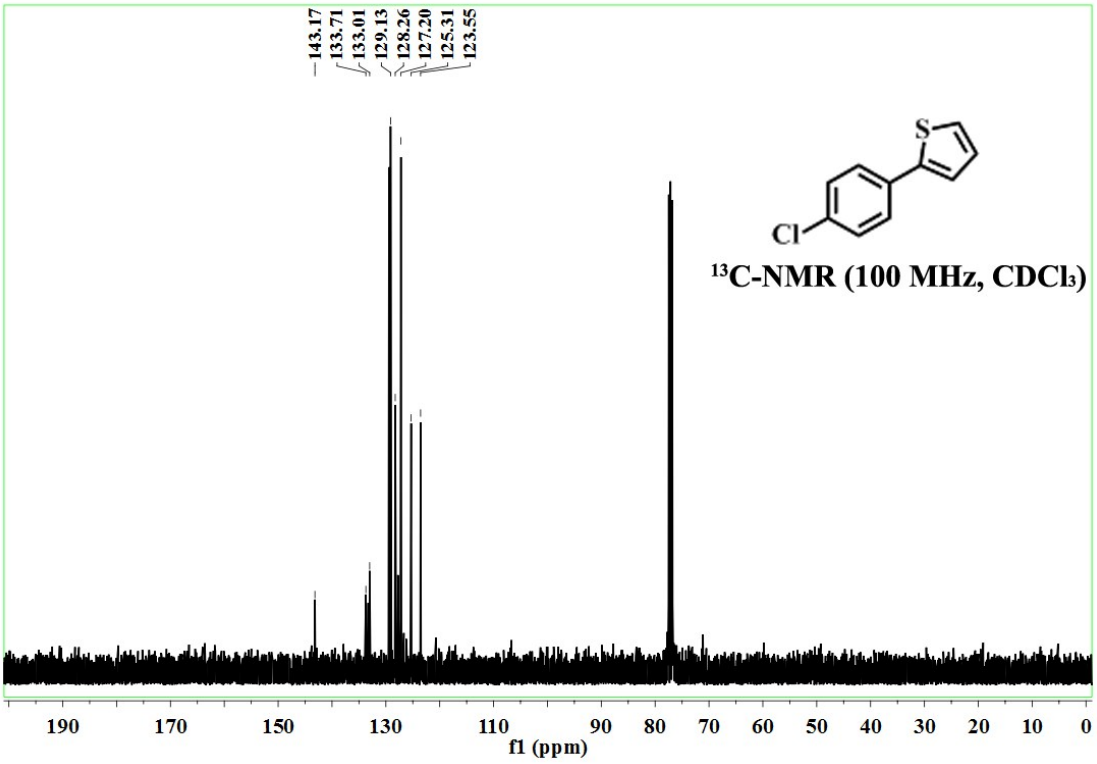

2-(4-Bromophenyl)thiophen[12]

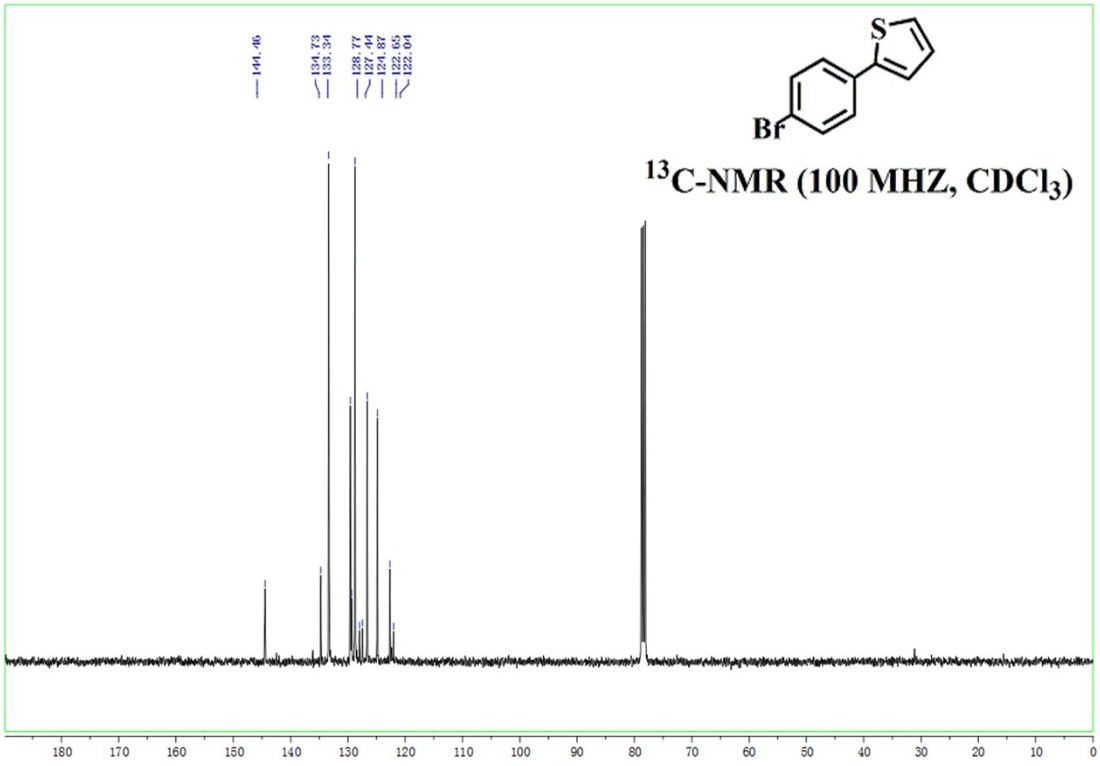

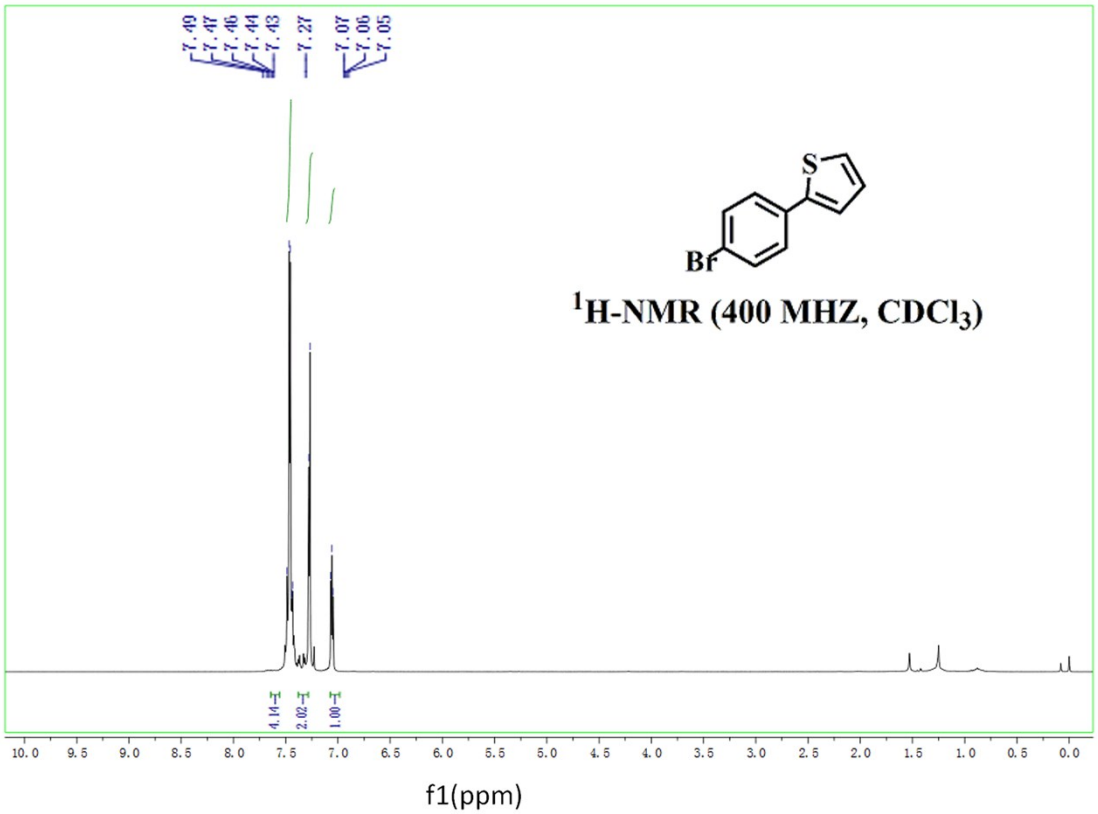

2-(4-Fluorophenyl)thiophene

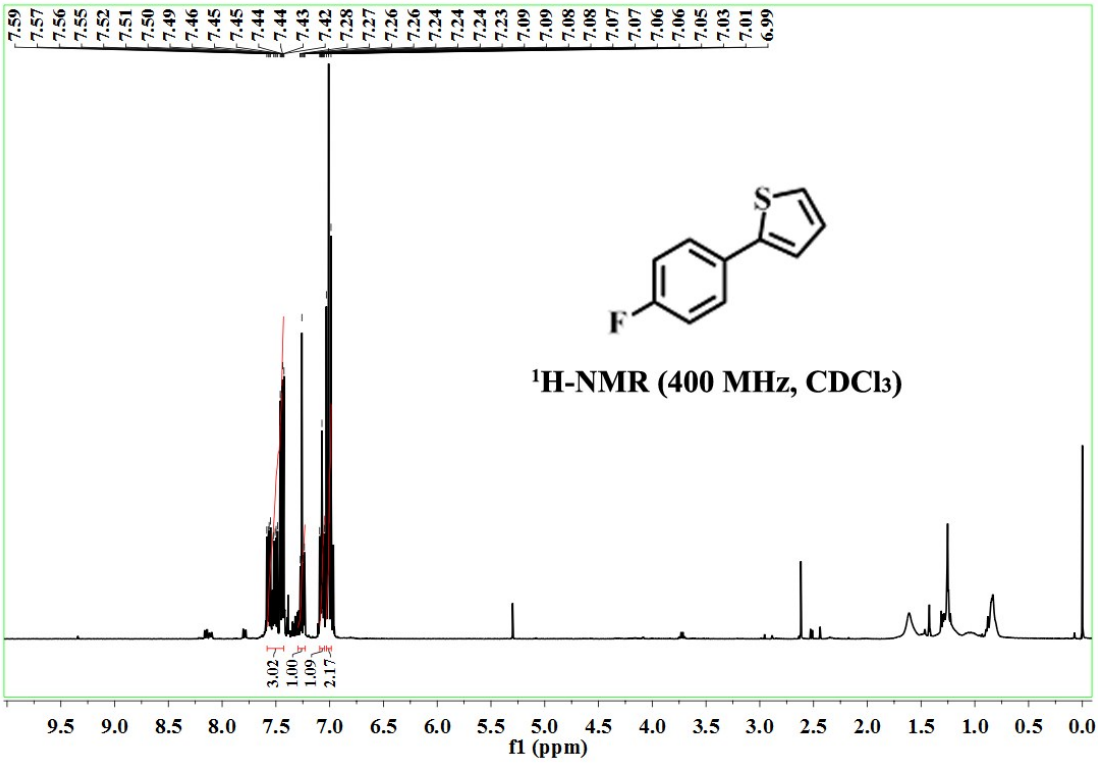

^{1}H-NMR (400 MHz, $CDCl_3$)

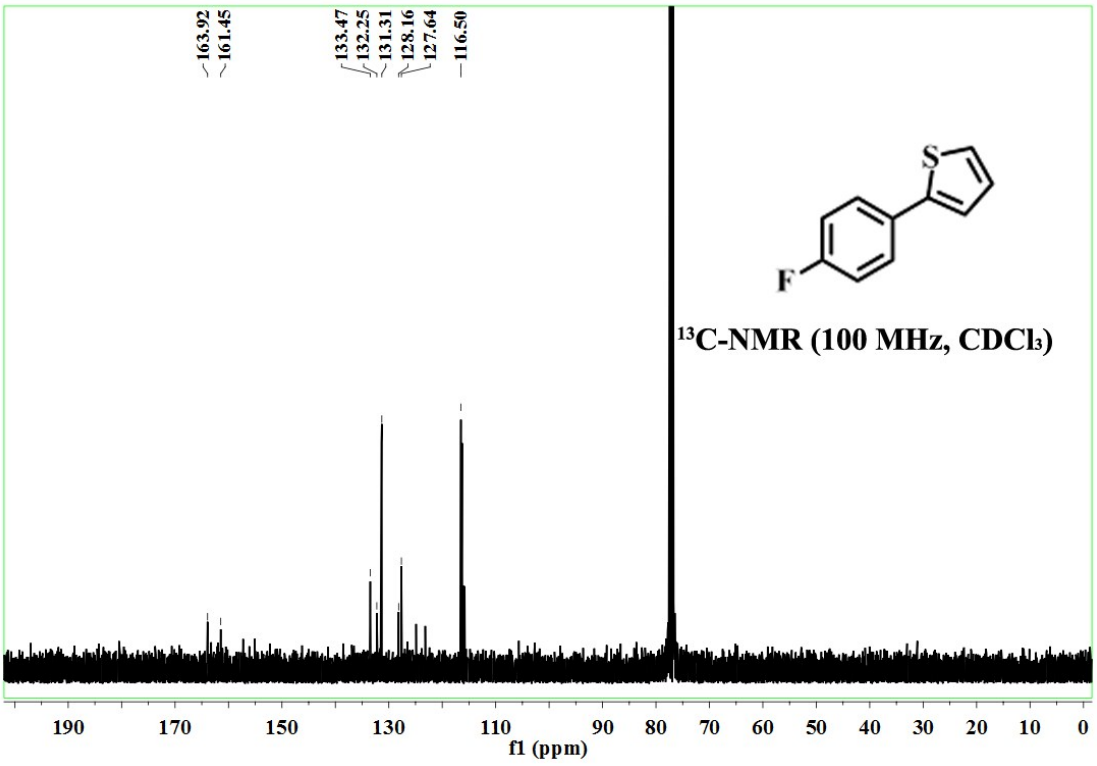

^{13}C-NMR (100 MHz, $CDCl_3$)

REFERENCES:

1 (a) W. J. Ong, L. L. Tan, S. P. Chai and S. T. Yong, *Chem. Commun.***,** 2015, **51**, 858-861; (b)Y. b. Li, H. M. Zhang, P. R. Liu, D. Wang, Y. Li and H. J. Zhao*, small* , 2013, **9**, 3336-3344.
2 C. Nethravathi and M. Rajamathi, *Carbon*, 2008, **46**, 1994.
3 Zh. G. Li, A. L. K. Lui, K. H. Lam, L. F. Xi and Y. M. Lam, *Inorg. Chem.*, 2014, **53**, 10874-10880.
4 E. L. Ding, J. Hai, T. R. Li, J. Wu, F. J. Chen, Y. Wen, B. D. Wang and X. Q. Lu, *Anal. Chem.* 2017, **89**, 8140-8147.
5 D. P. Hari, P. Schroll and B. König, *J. Am. Chem. Soc.,* 2012, **134**, 2958-2961.
6 L. H. Zhi, H. L. Zhang, Zh. Y. Yang, W. S. Liu and B. D. Wang, *Chem. Commun.,* 2016, 52, 6431—6434.
7 J. Zoller, D. C. Fabry and M. Rueping, *ACS Catal.*, 2015, 5, 3900-3904.
8 C. Y. Zhou, P. W. H. Chan and C. M. Che, *Org. Lett.,* 2006, **8**, 325-328.
9 S. K. Guchhait, M. Kashyap and S. Saraf, *Synthesis,* 2010, 1166-1170.
10 N. Kuhl, M. N. Hopkinson and F. Glorius, *Angew. Chem. Int. Ed*., 2012, **51**, 8230-8234.
11 N. Uchiyama, E. Shirakawa, R. Nishikawa and T. Hayashi, *Chem. Commun.,* 2011, **47**, 11671-11673.
12 J. H. Li, Y. Liang, D. P. Wang, W. J. Liu, Y. X. Xie and D. L. Yin, *J. Org. Chem.*, 2005, **70**, 2832-2834.